IOPscience iopscience.iop.org

Home Search Collections Journals About Contact us My IOPscience

On the character of defects in GaAs

This article has been downloaded from IOPscience. Please scroll down to see the full text article.

1989 J. Phys.: Condens. Matter 1 3213

(http://iopscience.iop.org/0953-8984/1/20/004)

View the table of contents for this issue, or go to the journal homepage for more

Download details:
IP Address: 94.79.44.176
The article was downloaded on 10/05/2010 at 18:11

Please note that terms and conditions apply.

J. Phys.: Condens. Matter 1 (1989) 3213–3238. Printed in the UK

On the character of defects in GaAs

S Dannefaer, P Mascher and D Kerr
Department of Physics, University of Winnipeg, Winnipeg, Manitoba R3B 2E9, Canada

Received 5 April 1988, in final form 12 October 1988

Abstract. Positron lifetime measurements on GaAs are presented and discussed and former measurements are reviewed. The limitations and appropriate criteria for adequate spectrum analyses are considered in detail. It will be shown that exceptionally good statistical accuracy is necessary for a reliable and consequential decomposition, and that source corrections are very important. Results for liquid phase electro-epitaxially grown GaAs conclusively show that the bulk lifetime for GaAs is 220 ± 1 ps. All other GaAs samples (grown by either the liquid encapsulated Czochralski method or by the horizontal Bridgman method) show variable bulk lifetimes up to 232 ps. Shallow traps are concluded to be the cause for this. The binding energy of positrons in such traps is estimated to be about 23 meV, and the trapping rate into deep traps from such shallow traps is found to be approximately five times smaller than from the bulk state. The shallow trap is likely to be substitutional boron or nitrogen. The shallow traps anneal mainly around 700 K. Deep traps are found in all samples, yielding lifetimes $\tau_D^I \simeq 260$ ps and 290 ps $\leqslant \tau_D^{II} \leqslant 315$ ps. These lifetimes occur in n-type, p-type and semi-insulating materials. The results support our earlier contention that the 290–315 ps components are due to divacancies and the 260 ps lifetime is due to monovacancies, in complex form with some impurity. The divacancy anneals around 620 K while the monovacancy–impurity complexes generally anneal around 800 K.

1. Introduction

The nature of defects in gallium arsenide is generally shrouded in much uncertainty and, at times, controversy. There are several reasons for this. First, the simple point-like defects are varied in character since there can be vacancies on both sublattices (V_{As}, V_{Ga}), anti-site defects (As_{Ga}, Ga_{As}), and interstitials (As_i, Ga_i). Reactions between such defects or with impurities and dislocations may well alter the relative concentrations of the point defects in rather an unpredictable fashion. Secondly, the experimental methods used to characterise the defects are only partially successful. Electron paramagnetic resonance (EPR) is difficult due to large hyperfine interactions with the nuclei resulting in broad resonance lines. Increased resolving power is obtained, however, in electron–nuclear double resonance (ENDOR) experiments. Infrared spectroscopy (IR) is powerful when defects can be detected via an interaction with light impurities, and deep-level transient spectroscopy (DLTS) is a most important technique in assessing the electronic level of a defect, but does not yield information on the physical make-up of the defect.

Positron annihilation is an attractive method in this context since it directly probes the vacancy and it is a microscopic method. The concentration level for a detectable response is ≃0.1 ppm (≃5×10^{15} cm^{-3}) which is a convenient level, and there are no restrictions regarding sample conductivity nor (in principle) sample temperature,

0953-8984/89/203213 + 26 $02.50 © 1989 IOP Publishing Ltd

contrasting the various restrictions placed on EPR, IR and DLTS.

One of the most serious shortcomings of the positron technique is that it is incapable of resolving directly positron lifetimes that differ by less than about 50 ps. This can be circumvented in many cases but nevertheless poses a recurring problem. Interstitials will not generally be directly probed, but can be detected via interstitial–vacancy interactions. Furthermore positrons will only be sensitive to defects in neutral or negatively charged states.

Since the very early positron lifetime measurements on GaAs (Fabri *et al* 1966, Noguchi *et al* 1972, Kuramoto *et al* 1973), which demonstrated effects from neutron irradiation and deformation, several other positron works have been done. Cheng *et al* (1979) found that the mean positron lifetime decreased upon annealing of as-grown GaAs around 250 °C and that electron irradiation increased the mean lifetime; Bharathi *et al* (1979) found a temperature-dependent lifetime in heavily Si-doped materials. Takai *et al* (1980) attempted decomposition of lifetime components in order to obtain more detailed information. Dannefaer (1982) reported on a systematic investigation of 12 semiconductors (including diamond). Kerr *et al* (1982) and Dannefaer *et al* (1984a, b) reported on low-temperature measurements and annealing experiments on as-grown GaAs in different states of doping. They found marked temperature effects which depended on the state of annealing. Uedono *et al* (1985) investigated dislocated GaAs finding different positron response from α and β dislocations as well as marked temperature effects. Hautojärvi *et al* (1986) performed the first low-temperature electron (3 MeV) irradiation experiments, and found a broad annealing range between 100 and 400 K which they interpreted as arising from the annealing of V_{Ga}. Doping effects have also been investigated by Dannefaer and Kerr (1986) who argued, based on annealing experiments, that impurity–vacancy complexes are common in GaAs regardless of conductivity type. Stucky *et al* (1986), on the other hand, found vacancies *only* in as-grown n-type materials and argued that these are arsenic vacancies. Corbel *et al* (1988) attributed charge state controlled positron lifetimes of V_{As} to $2-/-$ and $-/0$ levels situated 0.03 and 0.1 eV, respectively, below the conduction band.

Positron lifetime measurements have thus at least shown that vacancy-related defects are present in as-grown GaAs and that radiation produces more of such defects. There is also agreement that there are unusually strong temperature effects in the 20–300 K range. There are notable differences, however, among interpretations; we believe these differences are often of purely technical origin, stemming from the varying degrees of success in resolving lifetime components. In this paper we will devote considerable attention to these problems.

2. Experimental

Our positron lifetime measurements were conducted using two spectrometers having a time resolution of 230 and 255 ps (full width at half maximum). The less efficient spectrometer was used for room-temperature measurements where the coincidence count rate was 90–100 cps using a 4 μCi positron source. The more efficient spectrometer was used for low-temperature measurements to compensate for the larger detector separation. The coincidence count rate was here 50 cps using a 8 μCi positron source. Spectra were always accumulated to at least 6×10^6 total counts which for low-temperature measurements required 48 h per spectrum. Since the stability of the spectrometer is a problem over such long periods of time, temperature-sensitive elements

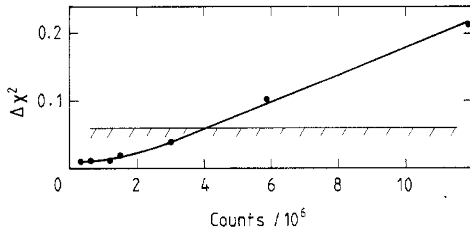

Figure 1. $\Delta\chi^2 = \chi^2$ (two-term) − χ^2 (three-term) as a function of total counts in each lifetime spectrum for Cd-doped GaAs. The horizontal line at 0.06 indicates the statistical uncertainty in χ^2.

(including the MCA board) were stabilised to within ±0.2 °C. The typical time jitter of the overall system was ±2 ps over a 48-h period. The positron sources were deposited directly on the samples in order to avoid a source contribution from backing materials. Furthermore, the source strength was kept very low again to avoid source contributions. Experiments on identical samples were occasionally conducted on both spectrometers and, as should be, identical results were obtained. Because different accumulation times were involved due to the different efficiencies of the spectrometers, this shows that no spurious effects arise due to time drifts of the spectrometers. The source contribution problem was investigated separately by using one sample set and adding source material in steps of about 2 μCi up to about 8 μCi of activity. No difference between the lifetime spectra could be seen from the computer analyses, but at larger source strengths, however, trends were obvious as a function of source strength. For these reasons our maximum source strength was only 8 μCi and no source correction was employed in the computer analysis of the data. We would like to point out that employing sources of strength 30 μCi can lead to a drastically different analysis (and hence misleading physical interpretation) compared to the spectrum obtained with only 4 μCi. It is not difficult to understand this since one finds that the lifetimes in GaAs are rather close together, so even minute additions (e.g. 2%) of a source contribution may alter the balance between the individual components.

The analysis of the spectra was performed using the codes developed by Kirkegaard and Eldrup (1974). The resolution function was determined by least-squares fitting to each lifetime spectrum. The parameters for the two Gaussians used to approximate the resolution function showed very little variation (±1 ps) during weeks of operation.

The spectra were then analysed assuming different numbers of lifetimes in the spectra. For the usual 6×10^6 or more counts in each spectrum it was never possible to obtain a good fit using only one lifetime component; the normalised χ^2 value was in excess of 10(!), whereas for a perfect fit one should find 1.00 ± 0.06. Two-term fits were not satisfactory either with χ^2 sums generally about 1.5 to 3. Three-term fits were generally acceptable, i.e., within 1.00 ± 0.06, but four-term fits were generally also possible giving (as expected) slightly better fits.

There is thus no point in discussing results from one- or two-term fits, but both three- and four-term fits should be considered seriously. Since the number of components obviously has ramifications for the physical interpretations one must consider the limits of statistical accuracy for which various types of analyses are possible. To illustrate this point a series of measurements was done on one typical GaAs sample (Cd-doped) with varying numbers of counts starting as low as 0.25×10^6 and ending at 12×10^6.

In figure 1 is shown the difference between χ^2-values for two-term and three-term analyses ($\Delta\chi^2$ is thus χ^2 (two-term)-χ^2 (three-term)). The statistical uncertainty of each χ^2 value is ±0.06, which is indicated by the horizontal line in figure 1. On a purely statistical basis three- and two-term fits are equally acceptable as long as the count number is less than about 3×10^6. Only higher count numbers show the inadequacy of the two-term fit. In the present work we have routinely used at least 6×10^6 counts. The

Table 1. Lifetime results for GaAs : Cd (p-type) after source correction (390 ps, 7.2%). Two- and three-term fits are shown in the upper and lower parts of the table, respectively. χ^2-values for the three-term fits were within 1.00 ± 0.06. The results for 12×10^6 counts (see table 2) are identical to those for 6×10^6 counts. The average lifetime $\langle\tau\rangle$ is calculated from the three-term fits according to $\langle\tau\rangle = I_1\tau_1 + I_2\tau_2$.

Parameter \ N	0.3×10^6	0.6×10^6	1.3×10^6	1.6×10^6	3×10^6	6×10^6
τ_1 (ps)	230 ± 1	229 ± 1	230 ± 1	230 ± 0	229 ± 0	229 ± 0
τ_2 (ps)	1386 ± 106	1329 ± 70	1323 ± 52	1340 ± 48	1364 ± 35	1354 ± 25
I_1 (%)	98.5 ± 0.1	98.5 ± 0.1	98.6 ± 0.1	98.6 ± 0.1	98.6 ± 0.1	98.6 ± 0.1
τ_1 (ps)	194 ± 85	189 ± 104	224 ± 10	222 ± 10	203 ± 32	183 ± 20
τ_2 (ps)	250 ± 53	242 ± 37	311 ± 159	306 ± 106	251 ± 29	243 ± 7
τ_3 (ps)	1590 ± 205	1455 ± 128	1487 ± 130	1551 ± 121	1544 ± 70	1545 ± 44
I_1 (%)	35.8 ± 110.4	24.1 ± 97.1	91.3 ± 23.6	88.9 ± 21.8	44.3 ± 60.5	22.8 ± 15.5
I_2 (%)	63.0 ± 110.3	74.6 ± 97.0	7.5 ± 23.4	10.0 ± 21.7	54.5 ± 60.5	76.0 ± 15.5
$\langle\tau\rangle$ (ps)	230	229	231	230	229	229

results obtained from these analyses are shown in table 1. The two-term fits exhibit a dominant lifetime component of 229 to 230 ps with an intensity of 98.5%, rather independent of the number of counts, N. We note that the uncertainty on these numbers decreases steadily up to $\sim 6 \times 10^6$, but little change is achieved beyond this number. The three-term fits show that the 229 ps lifetime from the two-term fit is actually composed of two components with lifetimes around 180 and 250 ps. As expected, the three-term fits are very uncertain below 3×10^6 since, according to figure 1, there is no real statistical difference between two- and three-term fits. The average lifetime $\langle\tau\rangle$ agrees well with the 229 ps lifetime from the two-term fit as one may expect. The ability of separating individual lifetime components which differ by only about 70 ps has already been demonstrated (Dannefaer 1981) and the present results agree quantitatively with these earlier findings.

The importance of these investigations is that completely different *physical* interpretations result from the analyses. If, as usual, we attribute the very low-intensity, long-lived component to spurious effects, then if one only were to perform the two-term fits the conclusion would be that the material is perfect and that the 230 ps lifetime is the bulk lifetime. The three-term fit, on the other hand, shows that in actual fact there is a considerable defect component (the 243 ps lifetime) resolved reliably, however, only at 6×10^6 counts or more.

Having thus established the *need* for rather high total counts in a spectrum this brings us to source strength considerations. It is tempting to achieve such high counts by increasing the source strength to reduce the measuring time. We have found, however, that such a procedure should be avoided, since accurate source corrections become very important as the source strength becomes large. We illustrate again by measurements on GaAs : Cd (one of many investigations conducted in this respect). In table 2 are shown results from analyses with and without source correction. The source strength was 30 μCi, about six times the source strength usually employed. It is clear that even the resulting bulk and average lifetimes are significantly affected.

The way in which the source correction is obtained is first to obtain a fit with the weak source and then determine the correction for the strong source by demanding agreement between the two spectra since identical samples were employed. The source correction

Table 2. Source correction effects. The source correction was 390 ps with 7.2% for a 30 μCi source strength. The spectrum contained 12×10^6 counts.

Parameter	Without correction	With correction
τ_1 (ps)	237 ± 0	229 ± 0
τ_2 (ps)	929 ± 10	1324 ± 17
I_1 (%)	97.51 ± 0.02	98.61 ± 0.02
I_2 (%)	2.49 ± 0.02	1.39 ± 0.02
τ_1 (ps)	210 ± 4	183 ± 18
τ_2 (ps)	305 ± 10	243 ± 5
τ_3 (ps)	1442 ± 44	1545 ± 25
I_1 (%)	68 ± 5	23 ± 11
I_2 (%)	31 ± 5	76 ± 11
I_3 (%)	1.21 ± 0.05	1.17 ± 0.03
τ_B (ps)	233	226
$\langle\tau\rangle$ (ps)	240	229

clearly has a dramatic effect and since it may be necessary to change sources from time to time we simply avoid source corrections altogether by using weak sources.

The considerations presented in this section have shown the necessity for lifetime spectra of high quality ($\geqslant 6 \times 10^6$ counts) in order to perform a sensible decomposition. A further increase in the quality is rather impractical since this would require unacceptably long data accumulation times. The choice made here is a workable compromise, but even then there will be cases of unresolved lifetime components. The necessity for high counts within a reasonable measuring time should, however, not be achieved by means of large source strengths, since this leads to large source corrections, but rather by efficient spectrometers.

One final point regarding the width of the resolution function should be mentioned. Although we have not done extensive investigations in this regard, results for systems with an inferior resolution function of about 320 ps (50–80 ps worse than normally used) showed that it often was impossible to perform even three-term fits reliably. In other words, we must have both an efficient and a good time-resolving system.

Regarding the annealing of the GaAs samples it will be noticed that the maximum annealing temperature throughout is only 600 °C. This is so because we wish to avoid arsenic evaporation from the sample. The annealing ambient was nitrogen.

3. Results

Mainly two types of experiments were conducted: isochronal annealing experiments where the measuring temperature was room temperature, and measurements where the sample temperature was varied between 30 and 300 K.

GaAs samples were obtained from several different sources but most were grown by the liquid-encapsulated Czochralski (LEC) technique employing pyrolytic boron nitride (PBN) containers, and boron oxide as the encapsulant. Another type of GaAs was grown by the horizontal Bridgman method also using PBN containers. One final type of GaAs was grown at 850 °C by the liquid phase electro-epitaxial (LPEE) technique. This latter type was grown at MIT, and is of particular interest due to its low growth temperature and high purity. We will here report detailed results of seven different samples all of

Table 3. Particulars of samples investigated in this work.

Property \ Sample	I	II	III	IV
Growth condition	LPEE[a]	Ga-rich LEC[b]	LEC	As-rich LEC
Type (at room temp.)	p ($<5\times10^{14}$ cm^{-3})	n	Semi-insulating	Semi-insulating
Dopant concentration (cm^{-3})	No intentional doping	Se 5×10^{16}	Cr 10^{18}	No intentional doping
Heat treatment	As-grown (850 °C)	As-grown (1240 °C)	As-grown (1240 °C)	
Proposed vacancy complexes		$V_{As}\cdot Se$	$V_{As}\cdot Cr_{Ga}$	$As_{Ga}\cdot V_{Ga}$

Property \ Sample	V	VI	VII
Growth condition	As-rich LEC	HB[c]	HB
Type (at room temp.)	p	n	n
Dopant concentration (cm^{-3})	No intentional doping	Si 1×10^{17}	Si 1×10^{17}
Heat treatment	1200 °C 16 h + quench	As-grown (1240 °C)	1200 °C 16 h + quench
Proposed vacancy complexes	$As_{Ga}\,V_{Ga}$ + $V_{As}\cdot V_{Ga}\cdot$?	$Si_{Ga}\cdot V_{As}$	$V_{As}\cdot V_{Ga}\cdot Si_{Ga}$

[a] Liquid phase electro-epitaxy.
[b] Liquid encapsulated Czochralski.
[c] Horizontal Bridgman.

which have undergone annealing and, in selected cases, low-temperature investigations. The particulars of these samples are listed in table 3.

Before presenting the results in detail a general remark should first be made. Although it is true that four-term fits often were performed successfully, only two components were of physical importance. These were the shortest-lived component (τ_1) which had values less than 220 ps, and the τ_2-component with values generally in the 250–300 ps range. The remaining two components had values around 500 ps (τ_3) and 1200 ps (τ_4). The 500 ps component did exhibit small variations with annealing but the 1200 ps component did not. Although the 500 ps therefore must be considered as arising from some defect in the GaAs, its overall importance is small because at most 2% of the positrons annihilated in those defects. The 1200 ps component had even a smaller percentage (0.2%) that was constant throughout. The inclusion of these two weak components is important, however, in achieving goodness-of-fit values close to 1.00.

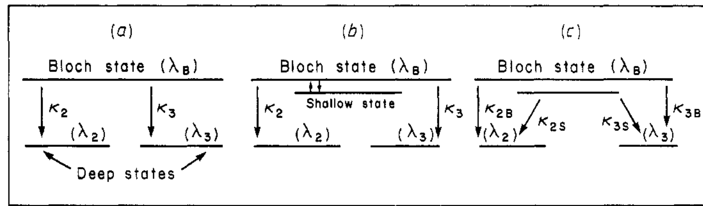

Figure 2. Different trapping models. (*a*) Trapping from Bloch state into two different vacancies (deep traps). (*b*) Addition of a shallow trap with trapping and detrapping (short arrows). (*c*) A shallow trap is considered effectively part of the Bloch state, and trapping into deep traps takes place also from the shallow state.

The inclusion of the τ_3 component influences the numerical value of τ_2 by up to 10 ps which is significant since we later on consider defects which yield lifetimes which differ by only 30 ps.

Before presenting the results we shall introduce the simple trapping model (West 1977) since part of the presented results are calculated from this model. We shall also present a variation of this model that will be used later on in connection with shallow positron traps.

In the simple trapping model (STM) one assumes that any positron occupies only one state, the Bloch state, at time $t = 0$. Trapping into deep states (vacancies) will then occur after $t = 0$ via the Bloch state with a rate which is proportional to the concentration of the deep state(s). In figure 2(*a*) this is shown for two different deep states. In this figure the horizontal lines designate the energy levels of the positron, the upper one being the Bloch state. The annihilation rate from this state is called λ_B while the annihilation rates in the two deep states are λ_2 and λ_3, both less than λ_B.

Solving the coupled differential equations governing the occupation probability of each of these three states, one finds their time dependencies according to

$$N_{\mathrm{STM}}(t) = \left(1 - \frac{\kappa_2}{\lambda_B - \lambda_2 + (\kappa_2 + \kappa_3)} - \frac{\kappa_3}{\lambda_B - \lambda_3 + (\kappa_2 + \kappa_3)}\right) \times \exp[-(\lambda_B + \kappa_2 + \kappa_3)t] + \frac{\kappa_2}{\lambda_B - \lambda_2 + (\kappa_2 + \kappa_3)} \exp(-\lambda_2 t) + \frac{\kappa_3}{\lambda_B - \lambda_3 + (\kappa_2 + \kappa_3)} \exp(-\lambda_3 t). \tag{1}$$

Note that at $t = 0$, N_{STM} equals one expressing that no annihilations have taken place at this time. The annihilation spectrum (or lifetime spectrum) is then given by

$$S_{\mathrm{STM}}(t) = -(\mathrm{d}/\mathrm{d}t)N_{\mathrm{STM}}(t) \tag{2}$$

since it is the disappearance of positrons which is detected in the experiments by virtue of the emitted γ-quanta.

Generally, the analytical form of an experimentally determined annihilation spectrum is given by

$$S_{\exp}(t) = \sum_i I_i \lambda_i \exp(-\lambda_i t) \qquad i = 1, 2, \ldots N \tag{3}$$

where I_i is called the intensity of the λ_i lifetime component. Values of I_i and λ_i are determined by least-squares analysis assuming N components. This analysis does not

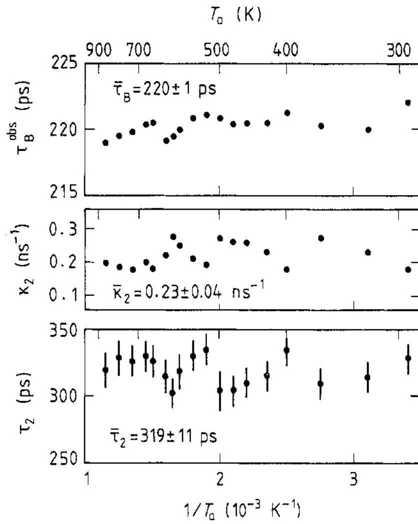

Figure 3. Lifetime results for LPEE-grown GaAs as a function of isochronal annealing temperature, T_a. This material constitutes our reference.

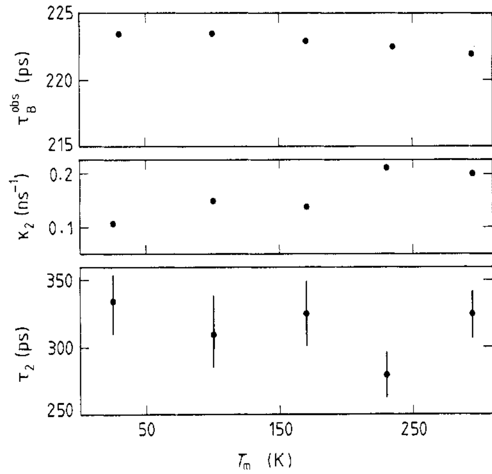

Figure 4. Lifetime results for as-grown LPEE GaAs as a function of measuring temperature, T_m.

assume the validity of the trapping model, only exponential decays, but if we equate $S_{exp}(t)$ with $S_{STM}(t)$ one finds

$$\kappa_2 = [\lambda_B - \lambda_2(1 - I_3) - \lambda_3 I_3]I_2/I_1 \tag{4}$$

and

$$\kappa_3 = [\lambda_B - \lambda_3(1 - I_2) - \lambda_2 I_2]I_3/I_1. \tag{5}$$

We note that the trapping rates κ_2 and κ_3, depend both on I_2 and I_3 (I_1 is given by $1 - I_2 - I_3$).

An important consequence of the trapping model is that the bulk annihilation rate can be calculated according to

$$\lambda_B = \lambda_1 I_1 + \lambda_2 I_2 + \lambda_3 I_3. \tag{6}$$

Since the bulk annihilation rate is a material constant (it refers to annihilation from the Bloch state), calculation of λ_B using the experimentally obtained values of λ and I therefore should yield constant λ_B-values regardless of the particular numerical values entering the right-hand side of equation (6).

We will now turn to the results, presenting them in the order I to VII as indicated in table 3.

3.1. LPEE GaAs

This type of GaAs is the most simple investigated so far. The results are shown in figure 3. Only three-term fits were possible and using equation (6), values of τ_B^{obs} ($\equiv 1/\lambda_B^{obs}$) were calculated from the experimental data. We note that τ_B^{obs} is constant (at 220 ± 1 ps), as is the vacancy-related τ_2-component. The value of τ_2 (319 ps) shows, as will be seen later, that vacancy complexes are responsible for this component. The trapping rate calculated from equation (4) using τ_B^{obs} = 220 ps is rather low. The fraction of positrons annihilating in the vacancy clusters is only 5%, so 95% of the positrons annihilate in the

bulk. We may also calculate the commonly used average lifetime according to

$$\langle\tau\rangle = I_1\tau_1 + I_2\tau_2 \tag{7}$$

omitting as usual the very small contribution (0.2%) from the very long-lived component of about 1200 ps. The value is constant at 225 ps.

It will be noted from figure 3 that only the τ_2-values are shown with error bars. These errors are the statistical errors provided by the computer fit. It is not straightforward to show error bars for the trapping rates nor the bulk lifetimes, since in calculating these values, parameters are used (equations (4) and (6)) which are correlated. We consider therefore the simple scatter exhibited by κ_2 and τ_B^{obs} as indicative of the true error. The as-grown LPEE-grown samples were also investigated as a function of measuring temperature in the 30–300 K range. From figure 4 there is an indication for a very weak decrease of τ_B^{obs} with increasing temperature. The trapping rate increases considerably, but there is no indication for a change in τ_2.

Although the present LPEE-grown material cannot be said to be perfect—it contains vacancy complexes—it is the most perfect material investigated so far, for which reason we will consider it as our reference material. We therefore equate the value of τ_B^{obs} in this sample with the true bulk lifetime τ_B. Recent systematic work on LPE-grown GaAs by Xiong Xing-Min (1986) shows a strong increase in defect concentration with growth temperatures between 750 and 950 °C. These defects give rise to a positron lifetime of 312 ± 11 ps.

3.2. *Ga-rich Se-doped LEC GaAs*

This sample shows a much more complicated behaviour (figure 5). Both three- and four-term fits are possible. When performing three-term fits τ_2 varied between 285 and 310 ps, while four-term fits effectively split this component into a well defined component close to 260 and a weak τ_3-component that varied between 350 and 450 ps. The fact that the four-term fit produced a well defined lifetime of 260 ± 15 ps while τ_2 in the three-term fit varied, and that this type of behaviour was common for many samples, make us prefer the four-term over the three-term analysis.

The results shown in figure 5 are for τ_2 fixed at 260 ps in the analyses as determined from the unconstrained four-term fits. Again we show τ_B^{obs} as calculated from equation (6) and using these values κ_2 and κ_3 are calculated from equations (4) and (5). The average lifetime $\langle\tau\rangle$ is calculated from equation (7) adding the term $I_3\tau_3$.

The values for τ_B^{obs} are significantly higher than for the LPEE-grown sample (figure 3) and show a variation with annealing temperature. We would like to stress that whether one uses a three- or a four-term analysis only alters the overall level of τ_B^{obs} by 1 ps, the four-term analysis yielding the lower values. The main reduction in τ_B^{obs} is centred around 770 K, while the main decrease in the κ_2 trapping rate is centred at 870 K. The lifetime of 260 ps has been found earlier (Dannefaer and Kerr 1986) in p-type GaAs (Zn-doped), but in the Ga-rich material the initial trapping rate is about 50% higher than in the (stoichiometric) Zn-doped samples.

We note that vacancy clusters as indicated by the ≃400 ps component appear to grow in size (longer lifetime) at the highest annealing temperatures while decreasing in number (κ_3 decreases). The average lifetime $\langle\tau\rangle$ exhibits changes linked *both* to the variations in τ_B^{obs} as well as to variations in κ_2.

3.3. *Cr-doped LEC-GaAs*

For this type of sample the long-lived (≃400 ps) lifetime component could not be found, so only three-term fits were possible. Figure 6 shows the results. τ_B^{obs} is initially rather

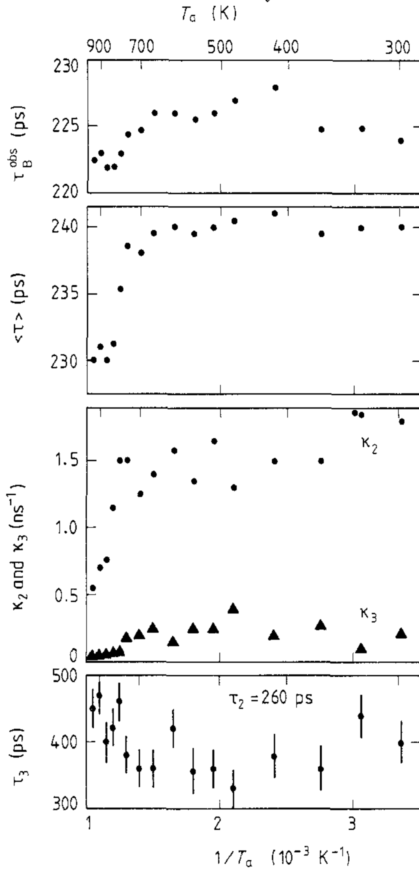

Figure 5. Lifetime results for LEC-grown Se-doped GaAs. $\tau_2 = 260$ ps was fixed in the analyses.

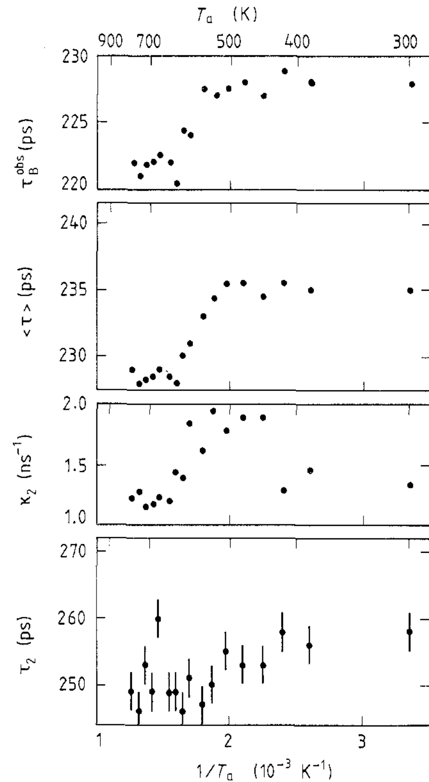

Figure 6. Lifetime results for LEC-grown Cr-doped GaAs.

high (228 ps) but decreases toward 222 ps centred at 590 K. The τ_2-component is initially 258 ps but decreases to 249 ps centred at 450 K, and simultaneously with this the trapping rate increases. The trapping rate then deceases centred at 590 K without any change in τ_2. The average lifetime $\langle\tau\rangle$ is remarkably insensitive to the low-temperature changes but does reflect the high-temperature variations. The 249 ps lifetime indicates a monovacancy albeit with a slightly reduced lifetime.

At-temperature measurements were also conducted on two sets of Cr-doped samples. One sample was from the isochronal annealing investigation after annealing at 770 K while the other sample was in the as-grown state. Both sets of samples were cut from the same wafer, but had nevertheless very different positron responses. As a function of temperature the annealed sample had a constant vacancy-related lifetime of 248 ps while the other one had a value of 281 ps. These lifetimes were then fixed in the analyses presented in figures 7 and 8. Despite the differences in τ_2 as well as the different levels of κ_2 both samples exhibit a decrease in τ_B^{obs} with increasing temperature. In figure 8 the value levels off at 232 ps at low temperature. Thew trapping rates increase with temperature in both cases, although not in a linear fashion as observed for the LPEE-grown material shown in figure 4.

It is illustrative that the average lifetime does not show as clear a temperature variation because of the opposing effects arising from a decrease of τ_B^{obs} and an increase of

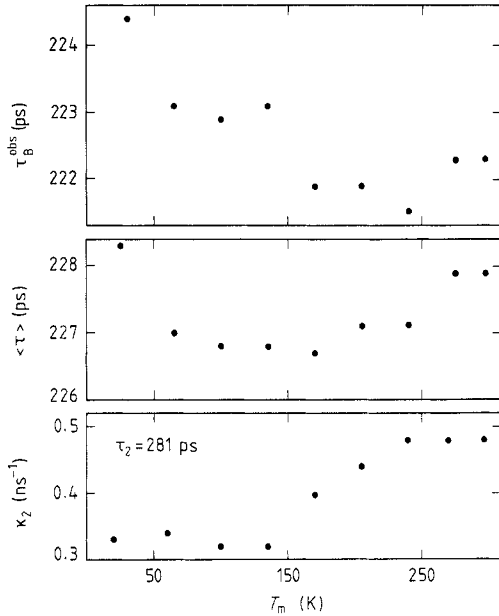

Figure 7. Lifetime results for as-grown Cr-doped LEC GaAs. τ_2 = 281 ps was fixed in the analyses.

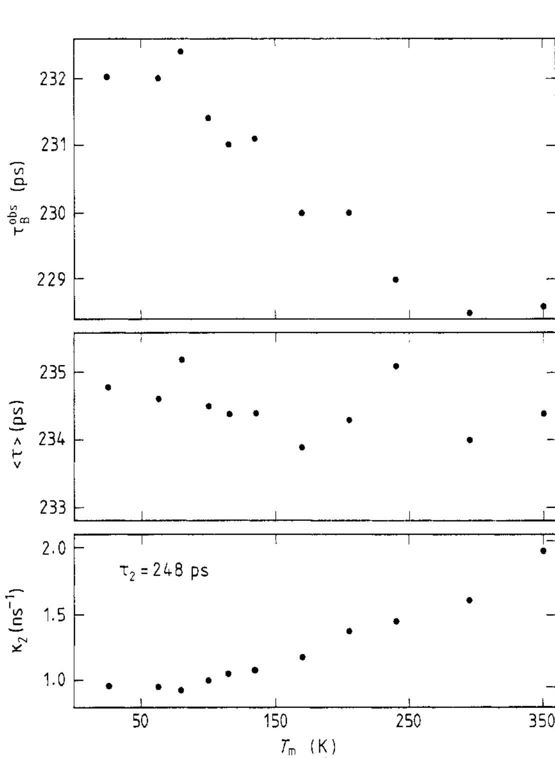

Figure 8. Lifetime results for Cr-doped LEC GaAs as a function of measuring temperature. This sample had undergone isochronal annealing up to 770 K (see figure 6). τ_2 = 248 ps was fixed in the analyses.

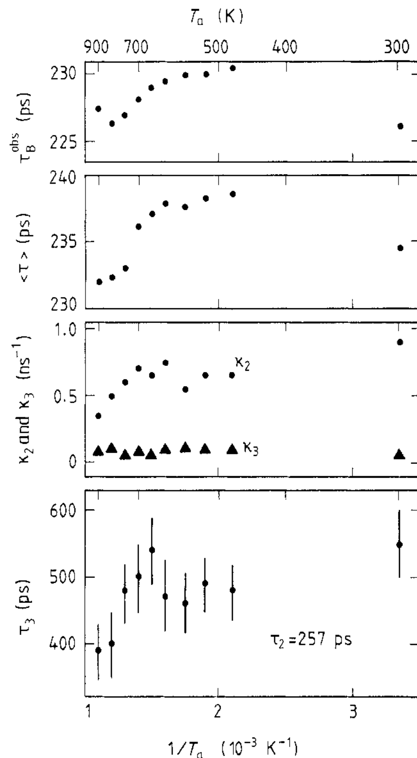

Figure 9. Lifetime results for semi-insulating (SI) undoped LEC GaAs. τ_2 = 257 ps was fixed in the analyses.

κ_2 with temperature. The levels of $\langle\tau\rangle$, however, reflect the different levels of κ_2 in figures 7 and 8.

3.4. As-rich LEC GaAs

This undoped semi-insulating GaAs sample was investigated first in the as-grown state where the concentration of the native mid-gap donor EL2 was 2×10^{16} cm^{-3} (Lagowski *et al* 1986). Four-term fits were again possible and yielded lifetimes very much like those observed in the Ga-rich, Se-doped sample (sample II). The τ_2 component did not change with annealing and had a value of 257 ± 10 ps, which was then fixed at 257 ps for the results shown in figure 9. The calculated τ_B^{obs} values are again high but show a clear decrease around 700 K. The trapping rate κ_2 (for the τ_2-component) decreases around 800 K, but no clear decrease takes place for the long-lived vacancy component (due to vacancy clusters). The average lifetime again shows variations coupled to variations in both τ_B^{obs} and κ_2. A partial account of these measurements as well as the following measurements has already been published (Dannefaer *et al* 1987) addressing the problem of the structure of the EL2 defect.

3.5. ITC-treated As-rich LEC GaAs

This sample is a variant of the sample just described. It was heated for 16 h at 1200 °C in an equilibrium arsenic ambient and then quenched in a few seconds to room temperature. The EL2 concentration is now an order of magnitude less than in the as-grown material (inverse thermal conversion—ITC, Lagowski *et al* 1986) and the material is slightly p-type after this treatment. In figure 10 are shown results from completely free four-term fits. The fits are left unconstrained since the τ_2-component changed during the annealing. The bulk lifetime is initially close to 230 ps but changes abruptly at 690 K to 225 ps. The trapping rate κ_2 decreases already at 625 K at which temperature half of the decrease has taken place. After annealing at 714 K an abrupt increase in κ_2 takes place, and the lifetime, τ_2, decreases sharply from the former level of 290 ps to 260 ps. This is the first time such an abrupt change (within 50 K) has been observed. We note that the trapping rate in this sample is about twice the value for the as-grown sample (figure 9), and that the lifetime initially is 290 ps, whereas it formerly was 257 ps.

3.6. Si-doped HB-grown GaAs

This sample is the only n-type material investigated in this work. As in most other samples a weak long-lived component is present (see insert in figure 11). The τ_2-component was constant at 267 ps (±5 ps) so this component was fixed at 267 ps in the analyses shown in figure 11. The main annealing stage of κ_2 takes place at 800 K as in most other samples. The fact that this material is n-type does not seem to effectuate any different behaviour as far as the positrons are concerned.

3.7. ITC-treated Si-doped HB-grown GaAs

This sample underwent the same thermal treatment as ITC SI GaAs described earlier (sample V), and 6×10^{16} acceptors cm^{-3} were introduced by this treatment. In figure 12(*a*) is shown a three-term fit after subtraction of the usual long-lived component of 550 ps with intensity 0.4%. The τ_B^{obs} is exceptionally high in this case, close to 240 ps, but

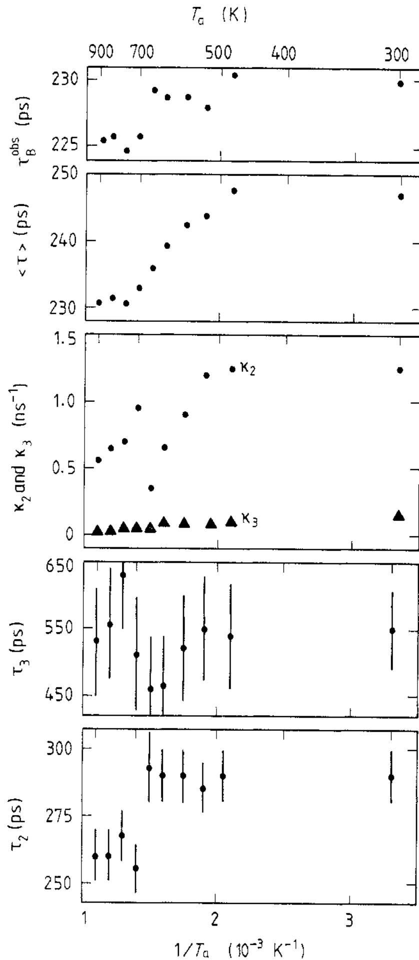

Figure 10. Lifetime results for ITC-treated GaAs (quenched from 1200 °C). The sample is identical to that shown in figure 9 except for the heat treatment.

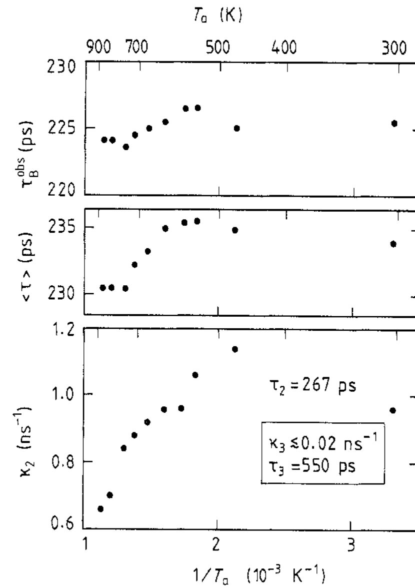

Figure 11. Lifetime results for horizontally Bridgman-grown Si-doped GaAs. $\tau_2 = 267$ ps was fixed in the analyses.

decreases rapidly at 700 K to a value of 225 ps at 870 K. The average lifetime decreases too, apparently in a stepwise fashion. The τ_2 lifetime is initially around 285 ps, which is slightly shorter than the 290 ps observed for ITC SI GaAs, dropping to 259 ps only at 873 K. This behaviour suggests that the τ_2-component is actually an average value of (at least) two lifetimes, so we assume that this average is composed of the 290 ps directly observed in SI GaAs and a contribution of 259 ps observed directly at the end of the annealing. This decomposition is of course not unique but appears reasonable in the context of the results for samples V and VI. The results from this type of analysis, shown in figure 12(b), behave as expected with the κ_3 trapping rate for the 290 ps component dominating at the lower annealing temperatures because τ_2 in figure 12(a) is close to 290 ps. At the higher annealing temperatures there is roughly an equipartition of the trapping rates, but there is no loss in total trapping rate. Only at 873 K does the 290 ps response disappear completely. We note, as has been stated before, that τ_B^{obs} does not change compared to the first fit and neither does $\langle\tau\rangle$. The total trapping rate ($\kappa_2 + \kappa_3$,

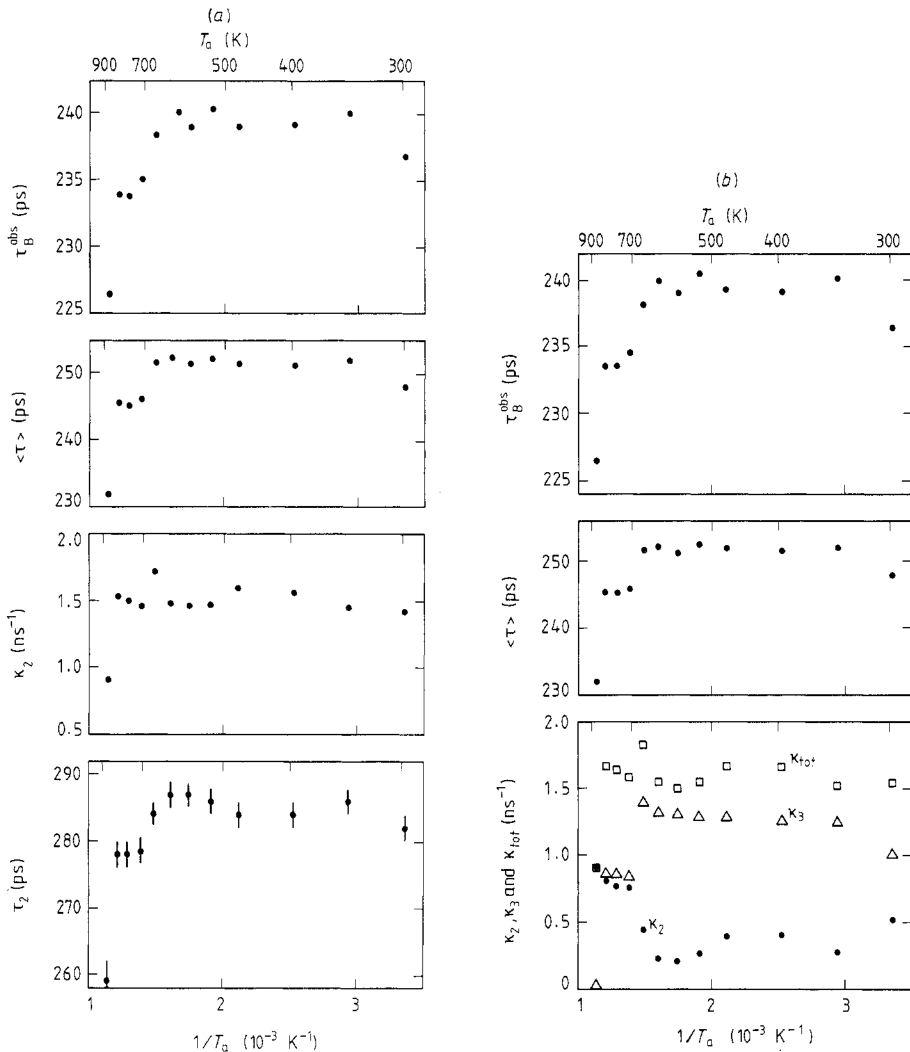

Figure 12. (*a*) Lifetime results for ITC-treated Bridgman-grown GaAs. The sample was identical to that shown in figure 11 except for the heat treatment. (*b*) Lifetime results for measurements shown in (*a*) but with $\tau_2 = 259$ ps and $\tau_3 = 290$ ps fixed in the analyses.

squares in figure 12(*b*)) is essentially the same as in figure 12(*a*), as it should be.

4. Discussion

The discussion will be divided into two main sections. The question of the bulk lifetime and shallow traps will be considered in § 4.1, and in § 4.2 the deep traps will be discussed. The section will be divided into three parts. In § 4.2.1. we will establish the association of the found lifetimes with particular vacancy types and give an interpretation of the observed annealing characteristics. In § 4.2.2 defect concentrations are estimated, and finally, in § 4.2.3 charge-state effects are briefly discussed.

4.1. Bulk lifetime and shallow traps

The most fundamental quantity one would like to know without any doubt is the bulk lifetime. It is relative to this value one gauges other lifetimes and it is a value which

occurs in the calculation of trapping rates and hence, ultimately, defect concentrations. Already at this point there are conflicting values. Stucky *et al* (1986) suggest a value of 233 ps, while Dannefaer *et al* (1984b) suggest a lower value of 220 ps. In fact, the first bulk lifetime suggested by Dannefaer (1982) was as high as 246 ps. It is illustrative to note that the same tendency towards shorter lifetimes also took place for silicon (and many metals) as one 'learns' the material. Some of the first reported bulk lifetimes in Si were around 240 ps (Sen and Sen 1974) but is now at 218 ps (Dannefaer *et al* 1986). It is not difficult to understand this type of development since low levels of defect concentrations or incorrect source corrections tend to increase the apparent bulk lifetime.

The data displayed for the LPEE-grown GaAs (figures 3 and 4) lead us to conclude that the bulk lifetime for GaAs is $\tau_B = 220 \pm 1$ ps. The reasons for this are that the value is independent of annealing temperature and that this sample is particularly free of defects. Furthermore, all other samples, even though they initially exhibited higher τ_B^{obs} values, also showed a decrease of τ_B^{obs} upon annealing; some samples (figures 5 and 6) reached values close to 220 ps.

The experimental value of 220 ps is smaller by 24 ps than predicted by the Brandt–Reinheimer model (1970), while the lifetime for silicon (218 ps) is longer by 16 ps. Recent and much more elaborate calculations by Puska *et al* (1986), Puska and Corbel (1988) and Puska *et al* (1988) could produce values of 229–235 ps for GaAs and 219–221 ps for Si by adjusting a 'gap' parameter E_g to about 0.2. In the Brandt–Reinheimer model this gap parameter was introduced to treat the valence electrons as *free* electrons albeit with an energy gap. The gap was selected to yield the experimentally determined high-frequency dielectric constant for the material in question (E_g is 0.40 for Si and 0.44 for GaAs), so E_g has nothing to do with the physical band gap. The introduction of this gap has the effect of increasing the positron lifetime only slightly (about 5%) compared to zero gap, which corresponds to a metal with the same electron density. Puska *et al* (1986) employed much more sophisticated calculations reproducing, for example, the experimental lifetime values for aluminium very well. The semiconductors, however, were treated again by introducing a gap, but in this case it was adjusted to yield the experimentally determined lifetimes rather than the high-frequency dielectric constant. The gap parameter was 0.2 in both cases and thus rather different from the values employed by Brandt and Reinheimer (1970), which is not surprising since different physical entities were being described by the same model. Still no physical significance should be attached to the gap parameter, nor its numerical values (even negative values could be acceptable).

In view of the rather simple model for the 'correction' to the positron–electron interaction in the semiconductor (reduced screening as governed by the gap parameter) it is actually gratifying to see that the theoretical calculations are quite close to the experimental values. We believe that discrepancies below the ±5% level (about 10 ps) can be caused by many contributions such as lattice relaxation (GaAs in particular), so that theory cannot realistically be construed as supporting one close value over the other.

On the purely experimental side of the problem, however, a 10 ps difference is of significance. Stucky *et al* (1986) claim to observe only the bulk lifetime in semi-insulating or p-type material since they could not detect any vacancies in these materials. The lifetime they do detect hence becomes (by definition) the bulk lifetime. But in their measurements they only had about 1×10^6 counts which, according to figure 1, makes the determination of an individual lifetime component very uncertain,

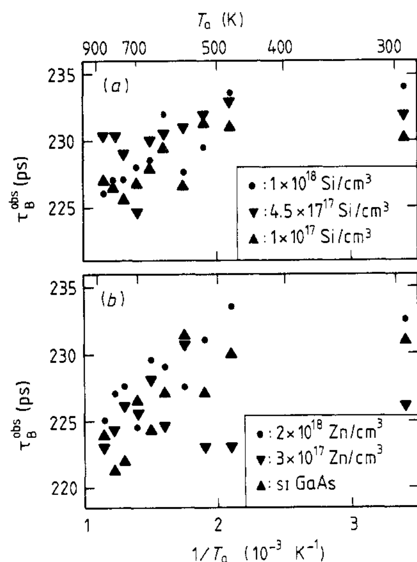

Figure 13. Observed bulk lifetimes calculated from data by Dannefaer and Kerr (1986). Results are for n-type LEC GaAs (panel *a*) and for p-type or semi-insulating LEC GaAs (panel *b*).

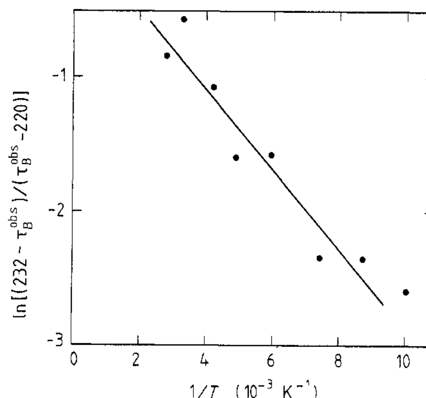

Figure 14. Arrhenius plot for the determination of the positron binding energy in shallow traps (cf equation 16) $E_B = 23$ meV.

so that in fact only an *average* lifetime can be obtained.

In the present measurements, where the vacancy lifetime can be separated because we employ 6×10^6 counts (cf again figure 1), the *average* lifetimes calculated on the basis of our measurements vary for the as-grown p-type, semi-insulating, and n-type materials between 225 and 240 ps (figures 5–11). They therefore agree numerically with the results of Stucky *et al* (1986), but demonstrate at the same time that the bulk lifetime is *not* 233 ps.

The importance of this is not only the correct determination of the bulk lifetime, but also that the existence of vacancies in p-type and semi-insulating GaAs can be deduced from positron lifetime measurements, provided sufficient accuracy is employed. To achieve this, good times resolution, high stability and low source strengths are necessary, as already explained.

We now turn to the variations of the observed bulk lifetime with annealing or measuring temperature. To substantiate the variations observed in this work we also show in figure 13 τ_B^{obs}-values based on a former set of measurements (Dannefaer and Kerr 1986). In all experiments, *except* for LPEE-grown GaAs, the bulk lifetime is above 220 ps, not only in the case of the samples investigated in this work, but also in the case of earlier samples as shown in figure 13. We observe the same type of behaviour of τ_B^{obs} with annealing temperature independent of whether the samples are n-type (Si-doped, figure 13(*a*)), p-type (Zn-doped, figure 13(*b*)) or semi-insulating (SI GaAs, figure 13(*b*)).

This suggests that a common defect is responsible for the variations in τ_B^{obs}; in other words τ_B^{obs} is actually a weighted average of the bulk lifetime (220 ps) and the defect lifetime. The omnipresence of this defect indicates strongly an impurity incorporated during the growth process. The dominant impurities would be substitutional boron, nitrogen, and, to a lesser extent, carbon (Thomas *et al* 1984) as incorporated during the growth from the pyrolytic boron nitride crucible and boron oxide encapsulant. For the LPEE-grown material which is grown only at 850 °C, this contamination

is much reduced if present at all. The above-mentioned impurities are undersized relative to Ga or As and will hence present a slight vacancy character constituting a shallow positron trap. The positron lifetime is likely to be rather close to the bulk lifetime judging from the detailed work on carbon decorated vacancies in iron (Puska and Nieminen 1982), but lacking theoretical calculations for the particular impurities considered here we can only suggest the usual argument that the positron wavefunction is only slightly localised around the impurity as for a shallow donor/acceptor state.

This qualitatively explains the salient features of the temperature dependencies displayed in figures 4, 7 and 8 in that the increase in τ_B^{obs} with decreasing temperature is due to an increased occupation probability of the shallow trap (corresponding to carrier freeze-out at low temperatures). The decrease in the trapping rate into deep traps with decreasing temperature is primarily explainable by the increased shallow trap population, although different mechanisms are possible as will be discussed below.

We will now quantify the above considerations, but in order to do so we must first consider the mechanisms by which positrons are being trapped in the presence of shallow traps.

In figures 2(*b*) and (*c*) are depicted two possible mechanisms. Figure 2(*b*) depicts the usual model which assumes that positrons at time $t = 0$ occupy *only* the Bloch state (bulk state) and that the shallow state is fed by the trapping rate κ_{ST} (short down-arrow) but is also depopulated by the detrapping rate δ_{ST} (short up-arrow). Trapping into one of the deep states *only* takes place via the Bloch state with the rate κ_2 and no detrapping is assumed to take place from a deep state. At low temperatures where $\delta_{ST} = 0$, *three* lifetimes should therefore emerge experimentally: the Bloch state depopulation lifetime ($1/\tau_1 = 1/\tau_B + \kappa_{ST} + \kappa_2$), the shallow-state lifetime ($\tau_{ST} \sim \tau_B$) and the deep-state lifetime τ_D.

In figure 2(*c*) is depicted another possibility, namely that at $t = 0$ *both* the Bloch state and the shallow trap are occupied according to a Boltzmann distribution and that trapping into one deep state can occur both from the Bloch state with rate κ_{2B} as well as from the shallow state with rate κ_{2S}. In this case only two lifetimes will occur. The 'bulk' state depopulation lifetime will be $\tau_1 = [(\tau_B^{obs})^{-1} + \kappa_{2B} + \kappa_{2S}]^{-1}$, where τ_B^{obs} is the weighted average of the true bulk lifetime and the shallow trap lifetime. The weighting depends on the shallow trap concentration and temperature. The other lifetime is then, as before, τ_D. This model predicts only two observable lifetimes in contrast to the three lifetimes in the former model.

To distinguish between the two possibilities an obvious route is to determine if two or three components are present at low measuring temperatures (low temperature means constant τ_B^{obs}). Higher-temperature measurements cannot reliably be used since detrapping (figure 2(*b*)) will modify the shallow trap lifetime as demonstrated by the high-temperature measurements on P-doped silicon (Mascher *et al* 1987a). We therefore used the at-temperature measurements on annealed Cr-doped GaAs, but only for measuring temperatures less than 90 K, since they did not show any temperature dependence (figure 8), to see if a lifetime, $\tau_{ST} \simeq 230$ ps, could be found. It was not possible to find such a component in an unconstrained fit, and when specifically constraining this component into the analysis χ^2-values emerged outside the statistically allowed range.

This purely numerical procedure is of course only one consideration and should only be construed as indicative. Another, and more physical, point is that the shallow trap ought to be treated only as an 'additional' bulk state as depicted in figure 2(*c*). To occupy the shallow trap only a few phonons need to be emitted to trap and likewise

only a few phonons have to be absorbed to detrap, so that the trapping and detrapping processes are fast compared to the case of deep traps. Hence, a thermodynamic equilibrium between Bloch states and shallow traps will be possible in contrast to the deep traps.

For these reasons, numerical as well as physical, we will proceed with the latter model to quantify it in the following way. The density of states in the Bloch state is N_B (here assumed temperature independent), while the density of shallow states is N_{ST} yielding the overall density of states:

$$N(E) \simeq \begin{cases} N_{ST} & 0 < E < kT \\ N_B & \Delta E < E < \Delta E + kT = E_{max} \end{cases} \tag{8}$$

where ΔE separates the shallow states from the Bloch state.

The fraction of positrons occupying the shallow trap is then

$$\alpha = N_{ST} \int_0^{kT} \exp(-E/kT)\,\mathrm{d}E \Big/ \int_0^{E_{max}} N(E) \exp(-E/kT)\,\mathrm{d}E \tag{9}$$

which yields, using the form of $N(E)$:

$$\alpha = [1 + (N_B/N_{ST}) \exp(-\Delta E/kT)]^{-1}. \tag{10}$$

The total annihilation rate then becomes

$$\lambda = \alpha\lambda_{ST} + (1 - \alpha)\lambda_B \tag{11}$$

which, for $\lambda_{ST} \sim \lambda_B$, yields to a good approximation τ_B^{obs} ($= 1/\lambda$ in equation (11)) as

$$\tau_B^{obs} = \alpha\tau_{ST} + (1 - \alpha)\tau_B. \tag{12}$$

The trapping cross section for trapping into deep states then becomes

$$\sigma = \alpha\sigma_{2S} + (1 - \alpha)\sigma_{2B} \tag{13}$$

where σ_{2S} is the trapping cross section from the shallow state and σ_{2B} is the trapping cross section from the bulk state.

The trapping rate into the deep state is then

$$\kappa_2 = \sigma C_D F(T) \tag{14}$$

where C_D is the deep-state concentration and $F(T)$ is a function that depends on temperature as $T^{1/2}$ in the case of diffusion-limited trapping. In the case of transition-limited trapping, $F(T)$ is actually independent of temperature. We may also write equation (14) in the form

$$\kappa_2 = \alpha\kappa_{2S} + (1 - \alpha)\kappa_{2B} \tag{15}$$

where symbols are defined in figure 2(*c*).

To proceed we now assume that the trapping rates κ_{2S} and κ_{2B} vary only slowly with temperature compared to the exponential dependence of α. This is certainly an approximation but at this stage we cannot do any better. In fact we know that there is a temperature dependence apart from the one arriving from α by virtue of the data for the LPEE GaAs shown in figure 4. To make the connection to experiment equations (10) and (12) yield

$$\ln[(\tau_{ST} - \tau_B^{obs})/(\tau_B^{obs} - \tau_B)] = -(\Delta E/k)(1/\mathrm{T}) + \ln(N_B/N_{ST}) \tag{16}$$

and from equations (12) and (15), α can be eliminated to yield

$$\kappa_2 = [(\tau_B^{obs} - \tau_B)/(\tau_{ST} - \tau_B)](\kappa_{2S} - \kappa_{2B}) + \kappa_{2B}. \qquad (17)$$

The Arrhenius-type equation (16) can be evaluated by noting first that at $T \leqslant 90$ K, τ_B^{obs} *saturates* at 232 ps (figure 8) so that this lifetime actually corresponds to τ_{ST} because of complete occupation ($\alpha = 1$) of the shallow traps. Secondly, $\tau_B = 220$ ps is found from the LPEE-type sample (figure 3). Figure 14 shows the plot as indicated by equation (16) from which one finds that the shallow positron trap is located about 23 meV below the bulk state. This numerical value confirms the basic assumption that the trap is indeed shallow and the value is typical for shallow dopant levels in semiconductors with a weakly localised hydrogen-like wavefunction. Extrapolating the data in figure 14 to $1/T = 0$ the value of N_B/N_{ST} is 1.16, so $N_{ST}/(N_B + N_{ST})$ is 0.45. The shallow traps comprise thus effectively 45% of all available bulk-type states in this sample.

We can estimate the radius of capture for the shallow traps as follows. Suppose the shallow traps have an activation volume of V_{ST} for trapping. Then the total volume is $N'_{ST}\,V_{ST}$ leaving for the bulk state the volume $(V - N'_{ST}\,V_{ST})$ where N'_{ST} is the number of shallow states and V is the total volume of the sample. The fractional number of bulk states is hence $(V - N'_{ST}V_{ST})/V_{at}$, where V_{at} is the atomic volume. In these terms and based on the conditions of equation (8), the ratio $N_{ST}/(N_{ST} + N_B)$ is equal to $N'_{ST}/(N'_{ST} + N'_B)$ and

$$N'_{ST}/(N'_{ST} + N'_B) = [1 + (V/V_{at}N'_{ST}) - (V_{ST}/V_{at})]^{-1}. \qquad (18)$$

The term $V/V_{at} \cdot N'_{ST}$ is simply $1/C_{ST}$, C_{ST} being the fractional concentration of shallow traps. Knowing the value of the left-hand side of equation (18) (0.45) then gives:

$$V_{ST}/V_{at} = (1/C_{ST}) - 1.22 \sim 1/C_{ST} \qquad (19)$$

or

$$r_{ST}/r_{at} \sim (1/C_{ST})^{1/3}. \qquad (20)$$

The actual concentration of the shallow traps is not known. It may well be of the order $10^{17}\,\mathrm{cm}^{-3}$ for boron (Thomas *et al* 1984). It we take $10^{17}\,\mathrm{cm}^{-3}$ as a typical concentration equation (20) yields $r_{ST}/r_{at} \sim 80$, which indicates very efficient trapping into the shallow traps.

The results for the Cr-doped sample shown in figure 7 cannot be used with confidence to extract a ΔE value since τ_B^{obs} is very close to τ_B.

As indicated by equation (17), κ_2 as a function of the experimentally determined value $(\tau_B^{obs} - \tau_B)/(\tau_{ST} - \tau_B)$ should yield a straight line with slope $(\kappa_{2S} - \kappa_{2B})$ and intercepts κ_{2B}. This type of plot is shown in figure 15 for the two Cr-doped samples shown in figures 7 and 8.

The high-valued κ (right-hand scale) yield a reasonably straight line from which we find $\kappa_{2S}/\kappa_{2B} \simeq 0.2$, or since trapping takes place into a *common* defect, the deep state:

$$\sigma_{2S}/\sigma_{2B} \simeq 0.2. \qquad (21)$$

The other Cr-doped sample (low κ, left-hand scale) exhibits the same trend but a numerical evaluation is not possible due to the large scatter of the data. These results indicate that the shallow traps modify significantly the 'normal' trapping process usually linked only to the Bloch (delocalised) state. The reduction by a factor of five in trapping cross section may appear high but presently we cannot comment further on

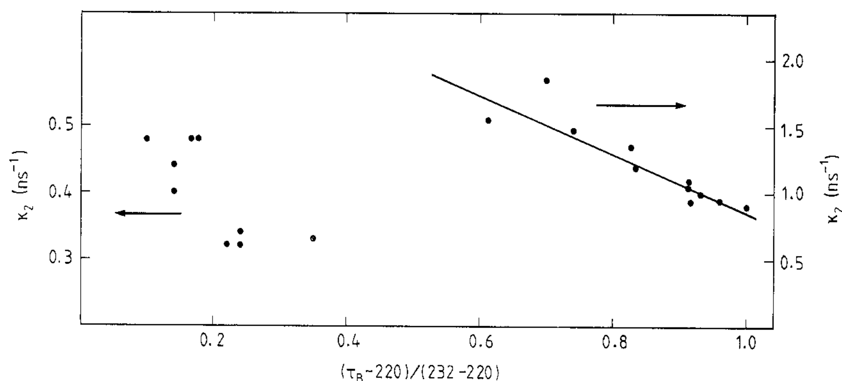

Figure 15. Plot for the determination of the relative trapping cross section into deep traps from either the Bloch state or from the shallow state (cf equation 17 and figure 2*c*).

this particular value. Further low-temperature measurements on suitable samples are certainly called for.

There is one straightforward implication, however. Shallow traps will reduce the overall trapping rate into deep states which in turn will lead to an underestimation of the deep-state concentrations. In the case of complete occupation of shallow states this underestimation would be a factor of about five!

We will return to this complication in connection with the deep states in § 4.2.2. The fact that shallow traps for the positrons in GaAs must be considered as a rule rather than an exception both broadens and complicates the applicability of the method. The positrons can monitor impurities which do not have any levels in the band gap, like boron and nitrogen. In doing so positrons have clearly shown that at least these impurities are not necessarily complexed with vacancies. Boron has also been investigated thoroughly by IR (Morrison *et al* 1974, Woodhead *et al* 1983, Gledhill *et al* 1984). In these works it was found that boron can be incoporated not only as electrically inactive B_{Ga} but also as an acceptor B_{As} which in turn can pair with a silicon donor. An anomalous reduction of the lattice parameter by residual impurity boron is undoped LEC-grown GaAs was observed by Okada and Orito (1988). The structure of the shallow positron trap may thus be rather complex.

The observed bulk lifetime decreased around 700 K in most samples, see figures 5, 6, 9–13 (variations of this temperature appear but we do not yet know the reason for this). This temperature of 'annealing' is not always linked to the annealing of deep states (vacancies), which would indicate that the shallow traps may anneal without the assistance of vacancies. We are not aware of other measurements which have identified an annealing stage in this temperature range.

We finally consider the Si-doped HB-grown sample (VI, VII, figures 11, 12*a*, *b*). The as-grown sample has τ_B^{obs} values in the usual range (<230 ps), but the ITC-treated sample has values of 240 ps. This, therefore, indicates that some shallow traps are present yielding a larger lifetime than the 232 ps hitherto discussed. This is not due to the fact that the sample is n-type since n-type materials in the as-grown state according to figures 11 and 13 yield the usual τ_B^{obs} values.

A possible explanation would be that pairs of impurities are quenched-in, since such pairs would have a larger overall free volume than isolated boron. Silicon is amphoteric so it can exist both as Si_{Ga} (donor) and as Si_{As} (acceptor). The low silicon concentration (1×10^{17} cm^{-3}) should mean that essentially all silicon is a donor

at room temperature, which should not affect the positrons at all. The positron measurements, however, suggest that due to the rapid quenching some Si_{As} has been retained in the form of $Si_{Ga} \cdot Si_{As}$ pairs (Theis and Spitzer 1984), i.e., at high temperatures there is a larger population of Si_{As}. Pairs such as $Si_{As} \cdot B_{Ga}$ are also possible positron traps but not $Si_{Ga} \cdot B_{Ga}$ since the former complex is an acceptor and the latter a donor. A complex like $Si_{As} \cdot B_{Ga}$ has been invoked by Morrow (1987) in explaining the carrier concentration versus silicon concentration in GaAs.

4.2. Deep states

4.2.1. Correlation between lifetimes and defect types. From the data presented in §§3.1–3.7 we can establish the following salient features.

(i) Positrons are trapped by defect in as-grown GaAs regardless of whether the samples are p-type, semi-insulating or n-type, and regardless of the method or the conditions of growth.

(ii) The trapped positrons yield lifetimes longer than the bulk lifetime. This means that the defect responsible for the trapping must have a lower average electron density than the bulk, i.e., they are vacancy-related. This follows from general positron annihilation theory (cf the review by West 1977). The fact that different lifetime values are found further means that the vacancy-related defects exist in different configurations (charge states or clusters).

(iii) The trapped positrons exhibit lifetime values in the range 250–267 ps (τ_D^I), in the range 290–315 ps (τ_D^{II}) and finally in a broader range of 430–550 ps (τ_D^{III}).

The narrow ranges of τ_D^I and τ_D^{II} strongly indicate that these two lifetimes correspond to two different but distinct vacancy-related defects, while the broad range for τ_D^{III} indicates varying but larger sizes of vacancy-related defects. Lifetimes in the above-mentioned ranges (τ_D^I and τ_D^{II}) have been found earlier by Dannefaer and Kerr (1986), Stucky *et al* (1986) and by Corbel *et al* (1988). Based on these observations we will now suggest an interpretation that relates τ_D^I to monovacancies, τ_D^{II} to divacancies, and τ_D^{III} to larger vacancy clusters.

For τ_D^I we note that the increase relative to the bulk value is 30–47 ps. In the case of silicon the increase from its bulk lifetime (218 ps) to the monovacancy value (270 ps) is 52 ps (Dannefaer 1987). This, by itself, suggests that τ_D^I is to be associated with a monovancancy in GaAs, and the recent theoretical calculations by Puska (1987) and Puska *et al* (1988) which yield increases of 36 and 39 ps for V_{Ga} and V_{As}, respectively, further substantiate our interpretation as well as that of Corbel *et al* (1988).

The increase for the τ_D^{II} lifetime is 70 to 95 ps relative to the bulk value. For silicon the increase for divacancies is 98 to 117 ps (Fuhs *et al* 1978) and calculations on GaAs by Puska and Corbel (1988) and Puska *et al* (1988) yield 87 to 92 ps. It would therefore seem that τ_D^{II} should be associated with divacancies, although Stucky *et al* (1986) and Corbel *et al* (1988) suggest that this lifetime is due to positron trapping by V_{As} in a singly negative charge state.

At this point it should be emphasised that the key difference between the results of Corbel *et al* (1988) and ours is that they claim to find trapping by vacancies only in n-type materials while we find trapping also in p-type and semi-insulating materials. As a consequence of their findings, Corbel *et al* (1988) are then forced to exclude the presence of V_{Ga} in as-grown GaAs and assign the trapping in n-type GaAs to different (negative) charge states of V_{As}. We strongly believe that their inability to observe

trapping in p-type and semi-insulating GaAs is caused by too low a statistical accuracy of the raw data as discussed earlier in this paper.

A most important question is the concentration of defects giving rise to the positron responses, since this has ramifications as to the physical character of the defects. In § 4.2.2 we will see that the concentration of monovacancies which give rise to a trapping rate of $1\ ns^{-1}$ is at least $1 \times 10^{17}\ cm^{-3}$ when dealing with overall neutral defects. In most samples the trapping rate is about $1\ ns^{-1}$ so if vacancies had been free (V_{Ga} or V_{As}) they should have been found by DLTS or Hall-effect measurements, since even concentrations of $\sim 10^{14}\ cm^{-3}$ are readily detected by these techniques. Furthermore, EPR could also have detected defects at such a level of concentration, at least V_{Ga}^{2-} following the interpretation of Goltzené *et al* (1986). We therefore suggest that the defects detected by the positrons should be of such a nature that they are not detected by DLTS, nor by EPR and should have little, if any influence on the carrier density. Interestingly, recent EPR studies by Bittebierre *et al* (1986) and by Weber *et al* (unpublished) have shown that at $T < 10$ K infrared irradiation makes possible the observation of defects at concentrations in excess of $10^{17}\ cm^{-3}$, much larger than hitherto thought. A defect type which can satisfy these restrictions would be a vacancy–impurity complex such as V_{As}–acceptor impurity, V_{Ga}–donor impurity, or V_{As} (V_{Ga})–isovalent impurity as suggested earlier by Dannefaer and Kerr (1986).

Further arguments for the existence of bound vacancies are based on the annealing behaviour of the divacancies. In SI GaAs they start to anneal (κ_2 decreases) at 525 K (figure 10), while in the Si-doped sample (figure 12*a*, *b*) they anneal first at 700 K. The latter annealing behaviour is peculiar, however, in the sense that, although the trapping rate for the 290 ps component (κ_3) decreases, the trapping rate for the 259 ps component (κ_2) increases by the same amount. There is therefore no net loss in vacancy concentration up to 850 K. The increased thermal stability in the Si-doped material may be understood by the complexing of a divacancy with a silicon impurity, just as in the case of monovacancies. Following the general idea of Van Vechten (1984) and Wager and Van Vechten (1987), the growth of the 259 ps component on the expense of the 290 ps component without any loss in overall vacancy concentration would indicate two different configurations of the three-body complex. The lowest energy configuration should then be nearest-neighbour vacancies plus the silicon yielding the 290 ps while during heating above about 700 K higher-energy configurations with vacancies not as nearest neighbours can be populated and frozen-in during the very rapid cooling to room temperature, to yield also the monovacancy response of 260 ps. No loss in overall trapping rate would take place.

The observed range of τ_D^I indicates a perturbation around the monovacancy and since τ_D^{II} also exhibits a range impurities appear to play a role here, too. The 319 ps component found in the LPEE-grown material, the 312 ps in LPE grown material (Xiong Xing-min 1986), the 315 ps found at $T < 100$ K in 300 MeV e^--irradiated GaAs (Mascher *et al* 1987b) suggest a particular defect configuration. These results amount to an increase from the bulk lifetime of 92–99 ps, very close indeed to the theoretically predicted value of 87–92 ps, so in these particular cases the response appears to be due to unperturbed divacancies.

The anchoring of vacancies by impurities has been adovacted above, but this could, of course, also be accomplished by dislocations. Normal dislocation densities in GaAs are about $10^4/cm^2$ which is, judging from the positron response in dislocated metals, three orders of magnitude too low to be detected. Also, plastically deformed Si has been investigated (Dannefaer *et al* 1983) showing that in silicon at least $1 \times 10^7\ cm^{-2}$

is needed to result in an observable positron response. Finally, dislocation-free GaAs (In-doped) has shown (Mascher *et al*, unpublished) that such samples do not differ in any material way from 'ordinary' samples. Grown-in dislocations seem therefore not to play any significant role in positron experiments.

Longer lifetimes, generally about 500 ps, and hence larger clusters are often present in as-grown LEC materials (except heavily Cr-doped GaAs) as seen in figures 5, 9–11. These large clusters are rather stable, persistent at least up to 900 K. An exceptionally large concentration of clusters was found in a sample (SI GaAs) which had first been quenched from 1200 °C (like the sample shown in figure 10) and then subsequently annealed at 850 °C in GaAs ambient. About 4% of the positrons annihilated in vacancy clusters, roughly four times as many as normally observed (Dannefaer *et al* 1987).

4.2.2. Defect concentrations. Estimation of the defect concentrations in as-grown GaAs involves several considerations. First of all we would like to have a sample where the positron–trap concentration has been found by independent means. We would also have to know the charge state of the defect since the positron trapping cross section depends strongly on charge. Third, we must consider the influence from shallow traps which would tend to decrease the observed trapping rate as shown in the first section of this discussion (equations (8)–(15)). Taking the latter 'correction' first, the trapping rate from the bulk state, κ_{2B}, into a deep state can be found, within the framework of the model for the effect of shallow traps, as

$$\kappa_{2B} = \kappa_2/[1 - \alpha(1 - \sigma_{2S}/\sigma_{2B})] \tag{22}$$

where σ_{2S} and σ_{2B} occur in equation (13) and α is determined by equation (12) as

$$\alpha = (\tau_B^{obs} - \tau_B)/(\tau_{ST} - \tau_B). \tag{23}$$

The lifetime parameters in equation (23) are determined experimentally so α can be calculated for the various samples. The ratio σ_{2S}/σ_{2B} is, however, only determined for the Cr-doped GaAs as ~0.2, but we will use this value also for all the other samples, assuming thus that all the shallow traps bring about the same reduction in σ_2. We further have to assume that τ_{ST} is the same (232 ps) for all shallow traps. In this way we can refer the experimentally observed trapping rate (κ_2) to a reference state, the Bloch state. It is clear that κ_{2B} will be larger than κ_2 by as much as a factor of five for the case of $\alpha_{max} = 1$, so the correction can be substantial.

In figure 16 are shown the results of this correction. The trapping rates are now substantially increased when referring only to the bulk state. Without this correction the defect concentration would have been underestimated by as much as a factor of three.

To estimate the defect concentrations it is important first to establish the charge state of the vacancy complex. Based on the at-temperature measurements of Cr-doped GaAs in this work and on the former work by Dannefaer *et al* (1984b) we conclude that these complexes are neutral since the trapping rate inceased with temperature, opposite the expected behaviour for negatively charged complexes (Dannefaer *et al* 1976, 1980). Also, for the divacancy we found no indication for a negatively charged state in ITC-treated GaAs. Taking then the trapping cross section simply as determined by the physical size of a vacancy (as done for metals where net charges are screened), the positron trapping cross section is 10^{-15} cm^2 and in the equation (Dannefaer *et al* 1976)

$$\kappa = C_D\, \sigma(2kT/m)^{1/2}, \tag{24}$$

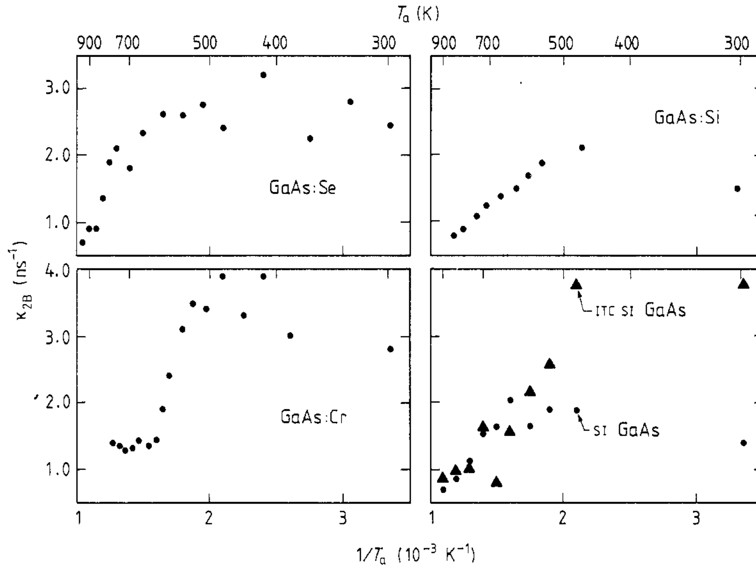

Figure 16. Trapping cross section for deep states referred solely to the Bloch state for the samples shown in figures 5, 6, 9, 10 and 11.

we find $(2kT/m)^{1/2} = 10^7\ \mathrm{cm\ s^{-1}}$ at room temperature, so that the defect concentration is

$$C_D = \kappa(\mathrm{ns}^{-1}) \times 10^{17}[\mathrm{cm}^{-3}]. \tag{25}$$

With κ values between 1 and 4 ns^{-1} (figure 16) the typical defect concentration in as-grown GaAs is then about 1–4 $\times 10^{17}\ \mathrm{cm}^{-3}$, an estimate in line with an earlier estimate without the use of equation (24) (Dannefaer and Kerr 1986).

We note that in the case of Se-doped GaAs the Se concentration is less than the estimated impurity–vacancy concentration of $\sim 2.5 \times 10^{17}\ \mathrm{cm}^{-3}$ by a factor of five, so other defect complexes must be present in a significant concentration. These could be Ga_{As} due to the Ga-rich growth condition, and the vacancy could then be V_{As}. In other words, this growth condition may well promote *both* the gallium antisite as well as the arsenic vacancy to accommodate the excess gallium.

We well realise that these estimates for the grown-in defect concentrations are higher by an order of magnitude than usually accepted, but we bring again to the attention the new EPR data which indeed indicate large defect concentrations apparently not detected by DLTS.

4.2.3. Charge state effects. In this final section we will briefly (due to the scarcity of data) discuss the only charge state effect so far found by positron annihilation.

This effect is indicated by the abrupt change in trapping rate in the ITC-treated SI GaAs at $1.6 \times 10^{-3}\ \mathrm{K}^{-1}$ (625 K) as seen in figure 16 (or figure 10 which does not inlcude the correction), simultaneously with an abrupt appearance of the 260 ps lifetime above this temperature. After the abrupt change the trapping rates for both the SI GaAs and the ITC-treated SI GaAs agree perfectly and the lifetimes are also the same. It should be mentioned that it was *not* possible to find a 260 ps lifetime component in lifetime spectra below 625 K even when attempting to fix the component in the analyses, and conversely it was not possible to find the 290 ps above 625 K.

This suggests that the monovacancy–impurity complex in SI GaAs ($As_{Ga} \cdot V_{Ga}$) is positively charged in ITC-treated SI GaAS (the material is slightly p-type) but upon annealing of the divacancies the Fermi level moves up towards the mid-gap crossing a $+/0$ level of $As_{Ga} \cdot V_{Ga}$ so the positron can become trapped.

5. Summary

This work gives new insight into important characteristics of positron–defect interactions in GaAs. Based on the behaviour of the bulk lifetime we have established first that the bulk lifetime is 220 ps in GaAs but that this lifetime is modified by the presence of shallow traps probably arising from boron, nitrogen or carbon impurities. Low-temperature measurements have indicated that the lifetimes for these traps are around 232 ps but may well vary when shallow-trap pairs can be formed. An analysis based on a modified trapping model for positron trapping indicates a positron binding energy of only 23 meV and, more importantly, that positrons in shallow traps have a reduced trapping rate into deep traps as compared with delocalised positrons.

Second, vacancies in GaAs can be detected by positron annihilation regardless of the position of the Fermi level. In as-grown materials the vacancies are complexed with impurities and their concentration is at least 10^{16} cm^{-3}. Such complexes result in a lifetime close to 260 ps, and the complexes are (when detected) neutral, but indication for a positively charged state of $As_{Ga} \cdot V_{Ga}$ has been found. Annealing of these complexes commences generally around 700 K, with $Cr_{Ga} \cdot V_{As}$ being an exception (590 K). Divacancies are not normally observed in GaAs but are found for low impurity concentrations or by means of rapid cooling from high temperatures (ITC treatment). They commence annealing around 500 K.

Furthermore, most materials also contain larger vacancy clusters at concentration levels of the order of 10^{16} cm^{-3}. These clusters are stable at least up to 900 K.

Acknowledgments

We are indebted to Dr J Lagowski for supplying the crucial LPEE-grown samples as well as the ITC-treated samples. This work was funded by the Natural Sciences and Engineering Research Council of Canada.

References

Bharathi A, Gopinathan K P, Sundar C S and Viswanathan B 1979 *Pramana* **13** 625
Bittebierre J, Cox R T and Molva E 1986 *Mater. Sci. Forum* Vol. **10–12** 365
Brandt W and Reinheimer J 1970 *Phys. Rev.* B **2** 3104
Cheng L J, Karins J P, Corbett J W and Kimerling L C 1979 *J. Appl. Phys.* **50** 2962
Corbel C, Stucky M, Hautojärvi P, Saarinen K and Moser P 1988 *Mater. Res. Soc. Symp. Proc.* **104** 475
Dannefaer S 1981 *Appl. Phys.* A **26** 255
—— 1982 *J. Phys. C: Solid State Phys.* **15** 599
—— 1987 *Phys. Status Solidi* a **102** 481
Dannefaer S, Dean G W, Kerr D P and Hogg B G 1976 *Phys. Rev.* B **14** 2709
Dannefaer S, Fruensgaard N, Kupca S, Hogg B and Kerr D 1983 *Can. J. Phys.* **61** 451
Dannefaer S, Hogg B G and Kerr D 1984a *Proc. 13th Int. Conf. on Defects in Semiconductors* eds L C Kimerling and J M Parsey Jr (Warrendale, USA: AIME) p 1029

Dannefaer S, Hogg B G and Kerr D 1984b *Phys. Rev.* B **30** 3355
Dannefaer S and Kerr D 1986 *J. Appl. Phys.* **60** 591
Dannefaer S, Kupca S, Hogg B G and Kerr D P 1980 *Phys. Rev.* B **22** 6135
Dannefaer S, Mascher P and Kerr D 1986 *Phys. Rev. Lett.* **56** 2195
Dannefaer S, Mascher P and Kerr D 1987 *Defect Recognition and Image Processing in III–V Compounds II*, ed. E R Weber (Oxford: Elsevier) p 313
Fabri G, Poletti G and Randone G 1966 *Phys. Rev.* **151** 356
Fuhs W, Holzhauer U, Mantl S, Richter F W and Sturm R 1978 *Phys. Status Solidi* b **89** 69
Gledhill G A, Newman R C and Woodhead J 1984 *J. Phys. C: Solid State Phys.* **17** L301
Goltzené A, Meyer B, Schwab C, David J P and Roizes A 1986 *Mater. Sci. Forum* **10–12** 1057
Hautojärvi P, Moser P, Stucky M, Corbel C and Plazaola F 1986 *Appl. Phys. Lett.* **48** 809
Kerr D P, Kupca S and Hogg B G 1982 *Phys. Lett.* **88A** 429
Kirkegaard P and Eldrup M 1974 *Comput. Phys. Commun.* **7** 410
Kuramoto E, Takeuchi S, Noguchi M, Chiba T and Tsuda N 1973 *J. Phys. Soc. Japan* **34** 103
Lagowski J, Gatos H C, Kang C H, Skowronski M, Ko K Y and Lin D G 1986 *Appl. Phys. Lett.* **49** 892
Mascher P, Kerr D and Dannefaer S 1987a *Phys. Rev.* B **35** 3043
—— 1987b *J. Cryst. Growth* **85** 295
Morrison S R, Newman R C and Thompson F 1974 *J. Phys. C: Solid State Phys.* **7** 633
Morrow R A 1987 *J. Appl. Phys.* **62** 3671
Noguchi M, Mitsuhashi T, Chiba T, Tanaka T and Tsuda N 1972 *J. Phys. Soc. Japan* **32** 1242
Okada Y and Orito F 1988 *Appl. Phys. Lett.* **52** 582
Puska M J 1987 *Phys. Status Solidi* (a) **102** 11
Puska M J and Corbel C 1988 *Phys. Rev.* B **38** 9874
Puska M J, Jepsen O, Gunnarson O and Nieminen R M 1986 *Phys. Rev.* B **34** 2695
Puska M J, Mäkinen S, Manninen M and Nieminen R M 1988 *Dept. of Physics, University of Jyvaskyla, Report* 8
Puska M J and Nieminen R M 1982 *J. Phys. F: Metal. Phys.* **12** L211
Sen P and Sen C 1974 *J. Phys. C: Solid State Phys.* **7** 2776
Stucky M, Corbel C, Geffroy B, Moser P and Hautojärvi P 1986 *Mater. Sci. Forum* **10–12** p 265
Takai O, Hisamatsu Y, Owada N, Iashimura H, Hinode K, Tanigawa S and Doyama M 1980 *Phys. Lett.* **76A** 157
Theis W M and Spitzer W G 1984 *J. Appl. Phys.* **56** 890
Thomas R N, Hobgood H M, Eldridge G W, Barrett D L, Braggins T T, Ta L B and Wang S K 1984 *Semiconductors and Semimetals,* ed. R K Willardson and A C Beer Vol. 20 (New York: Academic Press) p 1
Uedono A, Iwase Y and Tanigawa S 1985 in *Positron Annihilation*, ed P C Jain, R M Singru and K P Gopinathan (Singapore: World Scientific) p 711
Van Vechten J A 1984 *J. Phys. C: Solid State Phys.* **17** L933
Wager J F and Van Vechten J A 1987 *Phys. Rev.* B **35** 2330
West R N 1977 *Adv. Phys.* **22** 263
Woodhead J, Newman R C, Grant I, Rumsby D and Ware R M 1983 *J. Phys. C: Solid State Phys.* **16** 5523
Xiong Xing-Min 1986 *Phys. Energ. Fortis Phys. Nucl.* **10** 459 (Engl. Transl. 1987 *Chinese Phys.* **7** 455)